Nature of the Stranski-Krastanow Transition during Epitaxy of InGaAs on GaAs

T. Walther,[1] A. G. Cullis,[2] D. J. Norris,[2] and M. Hopkinson[2]

[1]*Institut für Anorganische Chemie, Universität Bonn, Römerstraße 164, D-53117 Bonn, Germany*

[2]*Department of Electronic and Electrical Engineering, University of Sheffield, Mappin Street, Sheffield S1 3JD, United Kingdom*

(Received 24 August 2000)

We report first quantitative measurements by energy-selected imaging in a transmission electron microscope of In segregation within an uncapped islanded $In_{0.25}Ga_{0.75}As$ layer grown epitaxially on GaAs. This layer has the lowest In concentration at which islanding occurs and, then, only after a flat ~3 nm alloy layer has been formed. In buildup by segregation at the surface of this initial flat layer is considered the driving force for islanding and, importantly, the segregation process introduces the characteristic delay seen before the Stranski-Krastanow transition. We observe strong inhomogeneous In enrichment within the islands (up to $x(\mathrm{In}) \approx 0.6$ at the apex) and a simultaneous In depletion in the remaining flat layer.

DOI: 10.1103/PhysRevLett.86.2381 PACS numbers: 68.65.Fg, 68.35.Dv, 68.55.Jk, 81.10.Aj

Misfit accommodation in strained epitaxial layers can take place through dislocation formation or through the occurrence of islanding and general surface roughness [1–4]. Often the growth mode transition from layer-by-layer growth to three-dimensional islanding occurs quite abruptly when a certain critical strain state is reached [5]. The latter so-called Stranski-Krastanow transition has been observed for many large-misfit strained layer system: It is driven by a type of morphological instability in an initially deposited flat layer [3,5–7] and is still the subject of detailed study. The islanding itself can yield self-organized arrays [8] of electronically active quantum dots suitable for advanced device applications, although the physics behind the islanding transition needs to be better understood to enhance the reproducibility and uniformity of the dot arrays produced. This fundamental understanding is addressed by the present Letter.

Calculations have shown that compositional variations within islanded alloy layers may be expected under certain growth conditions, either as a direct result of the strain [9] or due to different adatom mobilities on a rough surface [10]. Numerous experimental reports have speculated about lateral segregation in heteroepitaxial layers, mostly on the basis of results of indirect methods which measure effects related to the local chemistry of the layers [11–13]. High resolution transmission electron microscope (TEM) imaging [14] provides atomic-scale resolution, but maps only the local lattice parameter which depends on composition as well as on imaging conditions. The latter vary sensitively with, in particular, the degree of thin foil relaxation [15] although this has been modeled successfully using finite element calculations in plan-view investigations [16,17]. For the important cross-sectional geometry, however, the situation is much more complex because the thinned specimen foil can tilt and buckle locally [18]. This can lead to ambiguities of interpretation, and it appears understandable that some studies of InGaAs islands on GaAs have reported good agreement between simulated and measured lattice spacings [19] while others have attributed discrepancies to In concentrations either above [20,21] or below [22] the nominal values. A recent study which attempted to measure the local stoichiometry more directly by energy-filtered imaging with the In $N_{2,3}$ edge [23] failed to produce reliable data because of inadequate statistics and problems in image background correction.

In this Letter, we report the first direct elemental mapping of the strong lateral and vertical In compositional modulation of islanded uncapped $In_xGa_{1-x}As$ thin films grown on GaAs(001). The results highlight the importance of vertical segregation in the deposited flat layers immediately prior to island formation and confirm the compositional inhomogeneity of the islands ultimately produced. Layer growth took place by molecular beam epitaxy at 540 °C, the highest temperature at which In desorption can be considered insignificant, and at an In composition of $x \approx 0.25$, this being the lowest value at which the grown layers exhibit islanding behavior [5]. This choice of growth parameters ensured that the islanding transition was maximally delayed with the formation of an especially thick initial flat alloy sublayer. The overall growth was terminated when *in situ* reflection high energy electron diffraction showed that islands had just formed and the substrate was cooled rapidly after this point. A typical atomic force microscopy (AFM) image of the islanded surface is given in Fig. 1.

In the present work, energy-selected imaging (ESI) in a field emission gun transmission electron microscope (FEGTEM) has been applied to map the In and Ga distributions and the local specimen thickness in thin InGaAs layers. ESI has recently been developed as a powerful tool to map local compositional changes [24] as well as the absolute composition on the nanometer scale [25,26]. Previous studies have mostly dealt with capped island structures, since it is difficult to adequately protect the surface during cross-sectional specimen preparation by ion milling. We have bonded two cut pieces of the wafer with InGaAs islands face-to-face with epoxy resin, thereby producing a glue line of only 12 nm thickness. This made it possible to thin the specimen (after initial mechanical polishing) with low voltage argon ion milling

 © 2001 The American Physical Society

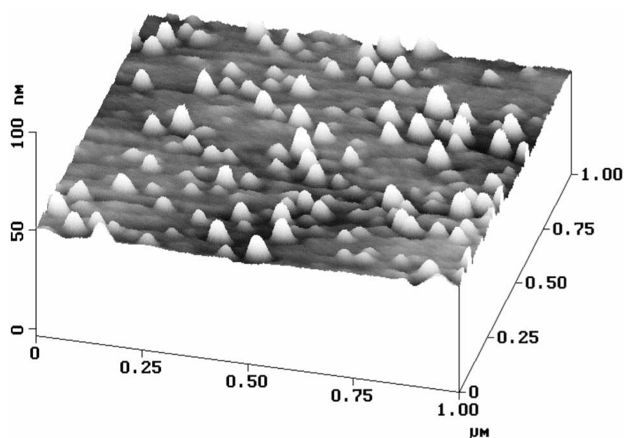

FIG. 1. AFM image of growth islands upon the $In_{0.25}Ga_{0.75}As$ layer.

from both sides until perforation without the ion beams actually disturbing the sensitive wafer surfaces.

The ESI work has been carried out using a Gatan imaging filter attached to a JEOL 2010F FEGTEM operated at a primary electron energy of 197 keV. Hartree-Slater calculations [27] have shown that the ratio, $\sigma_{\rm rel}$, of the ionization cross sections for the In $M_{4,5}$ to the Ga $L_{2,3}$ transition depends strongly on the energy window size and the collection angle if the windows are placed immediately behind the onsets of the corresponding edges, while this dependence is much less pronounced for integration windows centered 50 eV behind the onset of edges (see Fig. 2). For a beam convergence angle of $\alpha = 5$ mrad, a collection angle of $\beta = 37$ mrad, and energy windows of widths between $\Delta = 10$ and 80 eV, we then obtain $\sigma_{\rm rel} = 12.2 \pm 1.0$ [see Fig. 2(c)], and the cross section particularly of the delayed In $M_{4,5}$ edge is enhanced relative to

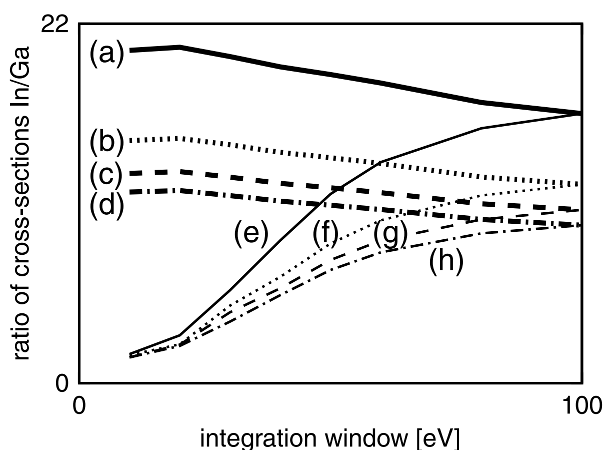

FIG. 2. Dependence of the ratio of inelastic scattering cross-sections of In $M_{4,5}$ to Ga $L_{2,3}$, for various collection apertures, β, on the width, Δ, of the integration window centered either 50 eV behind (a)–(d) or placed directly at the edge onset (e)–(h). Solid curves: $\beta = 7$ mrad; dotted: 20 mrad; dashed: 37 mrad; dot-dashed: 80 mrad. The experiments were performed using curve (c).

measurements directly behind the edge onset, thus improving the signal-to-noise ratio. The accuracy will mainly be given by that of the calculated scattering cross sections. While a comparison of experimental and theoretical oscillator strengths [28] indicates errors of 25%–30%, the scattering cross sections of both Ga $L_{2,3}$ and In $M_{4,5}$ edges are overestimated by a similar fraction, which almost cancels out in the calculation of their ratio. The cross correlation of images taken successively at different energies was performed to pixel accuracy after appropriate image filtering (low pass filtering to remove artefacts due to uneven illumination and high pass filtering for noise removal), then the background of the original pre-edge images was extrapolated using an inverse power-law least-squares fit and subtracted from the original post-edge images. Thus, net elemental maps were calculated for both elements, In and Ga. Since both elemental maps are spatially registered, their ratio, $r = I(\mathrm{In})/I(\mathrm{Ga})$ could be directly related to the indium composition $x = r/(r + \sigma_{\rm rel})$ [25,29]. These ratio maps exhibit negligible thickness [25] and diffraction effects, as the layers have been oriented edge-on about 3° off the $\langle 110 \rangle$ zone axis to avoid channeling. The thickness gradients measured close to the interfaces and surfaces of the specimen with InGaAs islands were small enough to neglect the influence of subpixel drift between the In and the Ga elemental maps on their ratio image. Also, the experiment was repeated 3 times on different areas, and the results were identical within the error bars.

Figure 3 shows a number of cross-sectional images and maps across a growth island. The epitaxial island lies on top of a flat InGaAs layer which has a full width at half maximum of ~3 nm, as seen from Fig. 4. The indium concentration in this flat layer region is significantly below the nominal composition [with a measured peak concentration of $x(\mathrm{In}) \approx 0.16$ rather than 0.25] and decreases further in the vicinity of the island [$x(\mathrm{In}) \approx 0.12$ at the base of the island]. While it is customary to describe a flat layer grown before islanding takes place as a "wetting layer," this is not a satisfactory description in the present case where substantial epitaxy of an InGaAs alloy has occurred. This observation gives important insight into the Stranski-Krastanow transition itself, as outlined below.

Examination of Figs. 3(f) and 3(g) shows that, first, the peak concentration of In in the epitaxial island is much greater than the nominal deposited composition. Furthermore, these figures demonstrate that the In composition within the island is not constant but increases from base to apex and shows a maximum of $x(\mathrm{In}) \approx 0.62$ along the vertical center line (see Fig. 4), while decreasing towards the periphery. Such compositions represent projected averages across the island in the electron beam direction: The actual peak In concentration will, therefore, be somewhat higher than the measured value given above. These direct composition maps are the first of their type to show such strong composition variations within an island and are in accord with scanning tunneling microscope (STM) studies presented recently [30]. Indeed, the measured local In

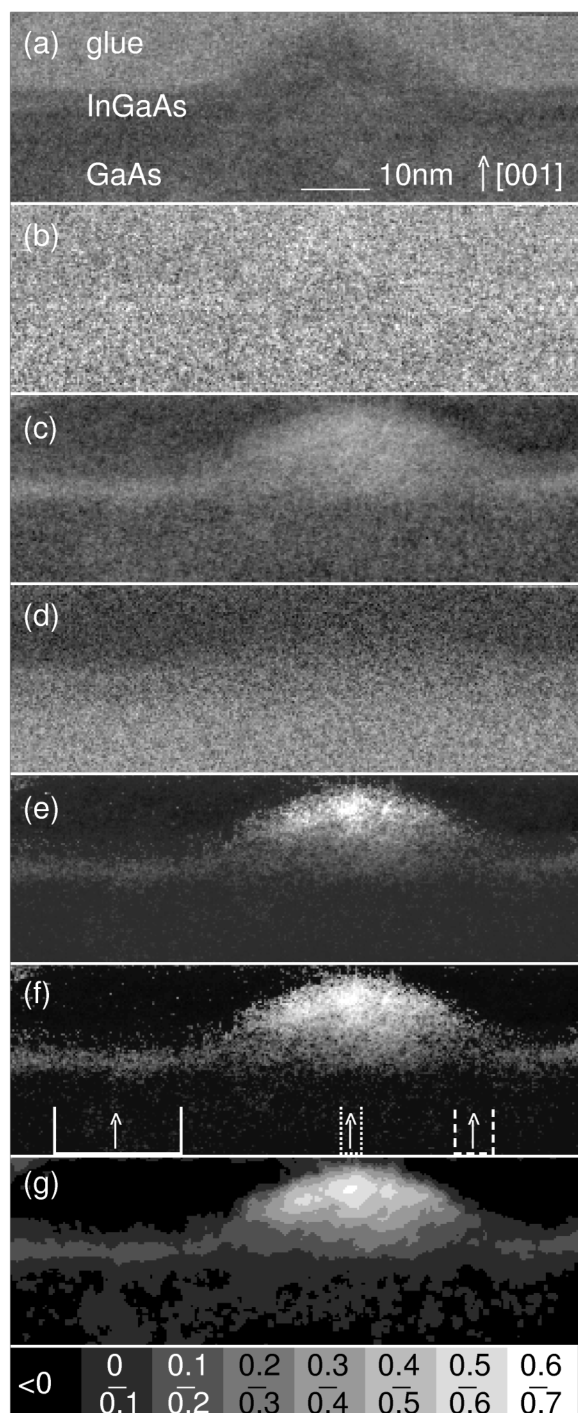

FIG. 3. Measurement of the chemical composition of InGaAs islands and wetting layers in cross section by ESI. Displayed are an elastic bright field image (a), a relative thickness map (b), a net In map (c), a net Ga map (d), and the In/Ga ratio map (e) from which an In concentration map (f) can be directly calculated. The gray-level map of (b) extends from 0.4 to 0.5 of the inelastic mean free path for electron scattering (~76 nm for InGaAs). For the map in (c), an improved multi-window method (with six pre-edge images between 300 and 425 eV and a least-squares fit to the *ln* of the intensities) was used. The sampling was 0.32 nm/pixel. (g) is a gray-level map of the In composition, calculated by averaging in (f) nearest-neighbor pixels and thresholding as indicated by the legend beneath. This effectively reduces the spatial resolution to 1 nm.

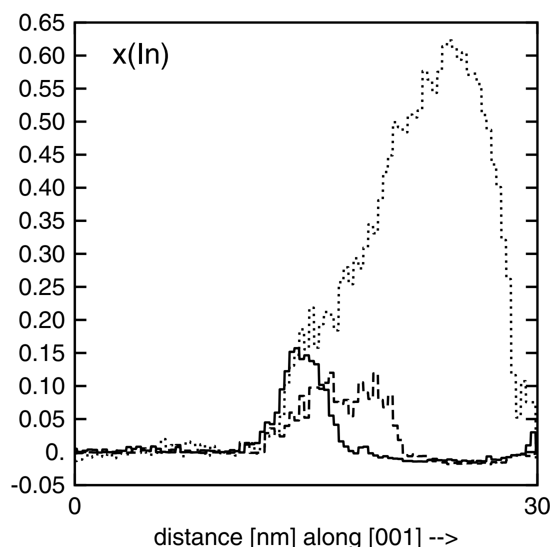

FIG. 4. Line profiles along [001] of the regions marked in Fig. 3(f) (solid line: 20 nm wide scan across the flat layer left of the island; dotted line: 3 nm wide scan across the center of the island; dashed line: 6 nm wide scan just at the right base of the island).

concentration values can be shown to be consistent, overall, with the deposition flux concentration of $x(\mathrm{In}) = 0.25$.

The above results indicate that the growth process proceeds in two key stages. First, a flat layer of epitaxial InGaAs alloy is formed and then, at a certain point, the transition to island formation occurs. Previous literature [3] has confirmed that this roughening is strain driven but, from the present results, it is clear that the critical strain is not achieved until a finite flat alloy layer has been deposited. It is proposed here that this islanding delay results from the need to build up a critical enhanced In concentration upon the alloy layer surface and that this process occurs by In segregation during the flat layer growth. This proposal has been correlated with theory by computing the expected rate of segregation of elemental In to the layer surface. The two-state exchange segregation model has been employed with In subsurface/surface activation and segregation energies taken to be 1.8 and 0.2 eV, respectively [31,32]. The assumed lattice vibration frequency was 10^{13} s^{-1}. The results of the calculations show that, within the limitations of the model and under the growth conditions employed here for the formation of a $In_{0.25}Ga_{0.75}As$ flat layer, it would be expected that ~3 nm of growth would take place before a stable surface In concentration of $x(\mathrm{In}) \approx 0.85$ could be established. Thus, the present work would indicate that the delay in island formation during Stranski-Krastanow growth is due to the need to build up such an In-enriched layer at the growth surface, resulting in a reduced In concentration in the underlying flat layer, as observed. Segregation enriched surface layers with lower In concentrations do not result in islanding since the present deposited flux has the lowest In concentration (~25%) for which islanding is actually observed [5]. For deposition fluxes with higher In concentrations,

surface In enrichment on the initial flat layer builds up more rapidly so that, for deposition of pure InAs, the flat (or wetting) layer is only <2 monolayers thick, as first suggested on the basis of TEM studies [33] and later confirmed by reflection high-energy electron diffraction [34] and AFM [35]. We note that the Stranski-Krastanow islanding transition is expected to have the same fundamental nature for all deposited In concentrations and, indeed, depends upon segregation in other heteroepitaxial systems.

The enhanced In concentration measured within the growth islands themselves results from the accumulation, from the layer surface, of In in these partially stress-relieved structures. Furthermore, the ESI measurements demonstrate that there is a reduced amount of In remaining at the flat layer surface around the island edges (Fig. 4, dashed curve). This is in accord with the presence of an accretion zone around each island, from which In has been extracted.

Lastly, it is important that the present direct composition measurements show the In distribution within a typical island. This is not uniform but exhibits a distribution apparently resulting from the preferential trapping of In atoms at the apex of the island, in accord with previous STM [30] and optical spectroscopy [36] measurements. The island apex is the location at which there is maximum lattice plane dilation [37], thus providing strain relief for the larger bonded In atoms. The form of the relaxation induces chemical potential gradients up the sides of each island and, in the surface atom diffusion fluxes during growth, these tend to separate In at the apex of the island from Ga near the base.

In conclusion, the present work has provided the first direct measurements, by elemental mapping, of the In composition in the early stages of InGaAs alloy growth on GaAs, demonstrating strong vertical and lateral In segregation. The delay in islanding characteristic of the Stranski-Krastanow transition is attributed to the requirement to form, upon an initially flat layer, a critically strained growth surface enriched in In by the process of (vertical) segregation. This work also confirms the inhomogeneous In distribution within the growth islands, which contain excess In near their apices.

The authors thank C. J. D. Hetherington for expert assistance with the FEGTEM operation and M. A. Al-Khafaji for recording the AFM image.

---

[1] S. Guha, A. Madhukar, and K.C. Rajkumar, Appl. Phys. Lett. **57**, 2110 (1990).

[2] D.J. Eaglesham and M. Cerullo, Phys. Rev. Lett. **64**, 1943 (1990).

[3] J. Tersoff and F.K. LeGoues, Phys. Rev. Lett. **72**, 3570 (1994).

[4] A.G. Cullis, A.J. Pidduck, and M.T. Emeny, Phys. Rev. Lett. **75**, 2368 (1995).

[5] A.G. Cullis, A.J. Pidduck, and M.T. Emeny, J. Cryst. Growth **158**, 15 (1996).

[6] D.J. Srolovitz, Acta Metall. **37**, 621 (1989).

[7] V.A. Shchukin and D. Bimberg, Rev. Mod. Phys. **71**, 1125 (1999).

[8] D. Leonard *et al.,* Appl. Phys. Lett. **63**, 3203 (1993).

[9] J. Tersoff, Phys. Rev. Lett. **77**, 2017 (1996); **81**, 3183 (1998).

[10] P. Venezuela and J. Tersoff, Phys. Rev. B **58**, 10 871 (1998).

[11] R. Sauer *et al.,* Phys. Rev. B **46**, 9525 (1992).

[12] Y.C. Kao, F.G. Celli, and H.Y. Liu, J. Vac. Sci. Technol. B **11**, 1923 (1993).

[13] H. Saitoh, K. Nishi, and S. Sugou, Appl. Phys. Lett. **73**, 2742 (1998).

[14] P.H. Jouneau *et al.,* J. Appl. Phys. **75**, 7310 (1994).

[15] M.M. Treacy and J.M. Gibson, J. Vac. Sci. Technol. B **4**, 1458 (1986).

[16] T. Benabbas *et al.,* J. Appl. Phys. **80**, 2763 (1996).

[17] X.Z. Liao *et al.,* Phys. Rev. Lett. **82**, 5148 (1999).

[18] T. Walther, C.B. Boothroyd, and C.J. Humphreys, Inst. Phys. Conf. Ser. **146**, 11 (1995).

[19] K. Tillmann *et al.,* Philos. Mag. Lett. **74**, 309 (1996).

[20] S. Kret *et al.,* Philos. Mag. Lett. **77**, 249 (1998).

[21] S. Kret *et al.,* J. Appl. Phys. **86**, 1988 (1999).

[22] A. Rosenauer *et al.,* Appl. Phys. Lett. **71**, 3868 (1997).

[23] R. Schneider *et al.,* Fresenius' J. Anal. Chem. **365**, 217 (1999).

[24] F. Hofer, P. Warbichler, and W. Grogger, Ultramicroscopy **59**, 15 (1995).

[25] T. Walther *et al.,* Mater. Sci. Forum **196–201**, 505 (1995).

[26] F. Hofer *et al.,* Ultramicroscopy **67**, 83 (1997).

[27] P. Rez, Ultramicroscopy **9**, 283 (1982); EL/P 3.0 software by Gatan Inc., Pleasanton, California.

[28] R.F. Egerton, Ultramicroscopy **50**, 13 (1993).

[29] T. Walther and C.J. Humphreys, J. Cryst. Growth **197**, 113 (1999).

[30] N. Liu *et al.,* Phys. Rev. Lett. **84**, 334 (2000).

[31] O. Dehaese, X. Wallart, and F. Mollot, Appl. Phys. Lett. **66**, 52 (1995).

[32] D.J. Norris *et al.,* J. Appl. Phys. **86**, 7183 (1999).

[33] F. Glas *et al.,* Inst. Phys. Conf. Ser. **87**, 71 (1987).

[34] H. Toyoshima *et al.,* Appl. Phys. Lett. **63**, 821 (1993).

[35] J.M. Moison *et al.,* Appl. Phys. Lett. **64**, 196 (1994).

[36] P.W. Fry *et al.,* Phys. Rev. Lett. **84**, 733 (2000).

[37] A.G. Cullis *et al.,* J. Vac. Sci. Technol. A **12**, 1924 (1994).